Photodetachment of hydrated oxalate dianions in the gas phase, $C_2O_4^{2-}(H_2O)_n$ ($n=3-40$): From solvated clusters to nanodroplet

Xue-Bin Wang, Xin Yang, John B. Nicholas,[a] and Lai-Sheng Wang[b]
Department of Physics, Washington State University, Richland, Washington 99352 and W. R. Wiley Environmental Molecular Sciences Laboratory, Pacific Northwest National Laboratory, Richland, Washington 99352

(Received 21 April 2003; accepted 19 May 2003)

Oxalate ($C_2O_4^{2-}$) is a common dianion, but it is not electronically stable as an isolated species due to the strong intramolecular Coulomb repulsion and can only exist as solvated species. We observed hydrated oxalate clusters, $C_2O_4^{2-}(H_2O)_n$ for $n=3-40$, using electrospray ionization of an oxalate salt solution and studied their energetics and stabilities using photodetachment photoelectron spectroscopy and theoretical calculations. We found that the smallest observable solvated cluster, $C_2O_4^{2-}(H_2O)_3$, has an adiabatic electron binding energy of ~0.0 eV, i.e., a minimum of three H_2O is required to stabilize $C_2O_4^{2-}$ in the gas phase. Theoretical calculations show that the first four waters bind tightly to $C_2O_4^{2-}$, each forming two H-bonds with $C_2O_4^{2-}$ peripherally without interwater H-bonding. The charges of the dianion were stabilized sufficiently that additional waters beyond $n=4$ form only single H-bonds with $C_2O_4^{2-}$ and interwater H-bonding was observed starting at $n=5$. The repulsive Coulomb barrier, characteristic of multiply-charged anions, was estimated from photon energy-dependent spectra for the smaller clusters and was found to decrease with increasing n. We observed that photoelectron intensities for features of the solute decreased as n increased, whereas detachment signals from the solvent became dominant for the large solvated clusters. This observation suggested that $C_2O_4^{2-}$ is situated in the center of the solvated clusters so that electrons detached from the solute were suppressed by the surrounding solvent layer. © *2003 American Institute of Physics.* [DOI: 10.1063/1.1590641]

I. INTRODUCTION

Because of its unique properties, water is the most important solvent in which many chemical and biological processes take place.[1] While a detailed understanding of its precise role is still being unraveled, it is clear that the existence of water shells around ions and biological molecules plays an important role. The water–water and water–ion interactions determine the microscopic hydration structures and eventually the bulk properties. The detailed understanding of bulk solutions requires knowledge of the energetic and dynamics of ion solvation. Extensive studies on bulk solutions have been pursued for several decades by a variety of experimental and theoretical techniques.[2–11] However, investigations of single ion hydration in the gas phase can provide molecular level information about the bulk, as well as providing model systems to verify theoretical methods and interaction potentials.

Thus, gas-phase ion cluster spectroscopy[12–14] combined with theoretical calculations[15–18] has become a popular research subject. Most experimental studies have been focused on the solvation of singly charged cations and monatomic halide anions.[19–25] Extending such studies to large hydrated clusters for complex anions (both singly and doubly charged) is imperative. The large clusters, containing tens of water molecules, provide opportunities to study the transition from solvated molecular systems to bulk solutions. However, to investigate solvated complex anions, particularly multiply-charged anions, is challenging. Unlike cations, which usually have large solvation energies and form internal state with a defined solvation shell,[2,5,12] anion solvation is more complicated. The delicate balance between the water–anion and water–water interactions determines the structure of the hydrated clusters.[15,16,19] One interesting issue of anion solvation is whether a given ion is sitting on the surface or in the inside of the solvent cluster in a finite system and how the solvation state evolves with the solvent cluster size.

Anion photoelectron spectroscopy (PES) is an important tool for studying the electronic structures of both aqueous solutions[26–29] and clusters.[20,30] Unlike infrared spectroscopy suitable for small hydrated clusters,[21,22,25,31,32] PES can yield electron binding energy and electronic structure information for any clusters. It has been used to study large hydrated iodide, $I^-(H_2O)_n$,[20] and hydrated electron, $(H_2O)_n^-$ ($n=2-69$).[30] Very recently, we have investigated several hydrated complex anions using PES coupled with an electrospray ionization (ESI) source. We have studied the hydration of NO_3^- with up to six water molecules,[33] and a series of dicarboxylate dianions, $^-O_2C-(CH_2)_n-CO_2^-$ ($n=2-10$) with one and two water molecules.[34] We have also investigated the hydration of a common inorganic dianion, SO_4^{2-}, with $n=3-13$ and showed that a minimum of three waters is

[a]Current address: Genentech, Inc., One DNA Way, South San Francisco, California 94080.
[b]Author to whom correspondence should be addressed. Electronic mail: ls.wang@pnl.gov

required to stabilize SO_4^{2-} in the gas phase.[35] A brief account of our study on large solvated SO_4^{2-}, as well as $C_2O_4^{2-}$, has been presented, demonstrating the transition from solvated clusters to behavior of nanodroplets.[36] A detailed account on the hydration of SO_4^{2-} with 3 to 40 waters has been reported.[37] In the current work, we present a detailed experimental and theoretical report of the hydration of $C_2O_4^{2-}$.

$C_2O_4^{2-}$ is an important inorganic dianion commonly found in solutions and solids. However, isolated $C_2O_4^{2-}$ is not stable with respect to autodetachment (to $C_2O_4^- + e^-$) because of the strong Coulomb repulsion between the two excess charges.[37] An interesting question concerns how many waters are needed to stabilize $C_2O_4^{2-}$ in the gas phase or how it is stabilized and solvated as a function of solvent numbers. Here we present a systematic PES study combined with theoretical calculations on $C_2O_4^{2-}(H_2O)_n$ ($n=3-40$) in the gas phase. The calculations focus on how the first few waters solvate and stabilize an isolated $C_2O_4^{2-}$ one H_2O molecule at a time. We find the minimum number of water required to stabilize a free $C_2O_4^{2-}$ is three. Both detachment features from the solute and the solvent were clearly observed. We found that the solute features decrease whereas the solvent features increase as a function of n. This observation suggests that $C_2O_4^{2-}$ locates inside the water clusters such that photoemission from the solute is suppressed by the solvent layer, analogous to behavior in bulk solution. Thus a transition from molecular clusters to bulk behavior is observed as a function of solvent.

II. EXPERIMENT

The experiments were carried out with a magnetic-bottle PES apparatus coupled to an ESI source. Details of the experimental apparatus have been given elsewhere.[39] Briefly, the $C_2O_4^{2-}(H_2O)_n$ clusters were produced from electrospray of a solution, containing 10^{-3} M $K_2C_2O_4$ desolved in a water/acetonitrile (15/85 ratio) mixed solvent at neutral *p*H. The anions produced from the electrospray were transported by a RF-only quadrupole ion guide and accumulated in a quadrupole ion-trap for 0.1 s before being analyzed by a time-of-flight mass spectrometer. Optimal moisture and careful control of collision-induced dissociation in the ESI source and during the subsequent ion transport to the ion-trap were critical for observing the oxalate–water solvated clusters. During the PES experiment, a given cluster was mass selected and decelerated before intercepted by a probe laser beam in the photodetachment zone of the magnetic-bottle photoelectron analyzer. In the current study, we employed three detachment photon energies, 157 nm (7.866 eV), 193 nm (6.424 eV), and 266 nm (4.661 eV). The experiments were done at 20 Hz with the ion beam off at alternating laser shots for background subtraction. Photoelectrons were collected at nearly 100% efficiency by a magnetic-bottle and analyzed in a 4-m long electron flight tube. The electron energy resolution of the apparatus is $\Delta E/E \sim 2\%$, i.e., 20 meV for 1 eV electrons. Photoelectron time-of-flight spectra were collected and then converted to kinetic energy spectra, calibrated by the known spectra of I^- and O^-. The electron binding energy spectra presented here were obtained by subtracting the kinetic energy spectra from the detachment photon energies.

III. THEORETICAL METHODS

We performed theoretical calculations on $C_2O_4^{2-}(H_2O)_n$ solvated clusters for n up to 6. Final geometries of all complexes were optimized using density functional theory, the B3LYP exchange-correlation functional[40] and the TZVP+ basis set. The TZVP+ basis set was derived from the DFT-optimized TZVP basis set[41] by addition of a diffuse *s* function to each H, and diffuse *s* and *p* functions to O and C. The exponents of the diffuse functions were obtained from an even-tempered extrapolation of the outer exponents of the original basis set. Frequency calculations were done to verify that the optimized geometries were stable points on the potential energy surface. We then obtained more accurate energies from single-point B3LYP calculations using the aug-cc-pVTZbasis set[42] on all oxygens, the cc-pVTZ basis set[43] on all hydrogens, and the B3LYP/TZVP+ geometries. The single-point energies were converged to 10^{-8} a.u. to insure accuracy. In order to locate the lowest dianion energy minima, ~10 initial geometries of each complex were first optimized at low levels of theory (typically RHF/3-21+G*). Many of the initial geometries optimized to the same final structure, generally giving ~3 geometries for use as input to the higher level optimizations. The geometries of the singly charged anions were optimized using the corresponding dianion geometries as starting points. We used GAUSSIAN 98 (Ref. 44) for all of the computations.

IV. EXPERIMENTAL RESULTS

A. Mass spectrum of hydrated oxalate clusters

A typical mass spectrum of $C_2O_4^{2-}(H_2O)_n$ from our electrospray source is shown in Fig. 1. The smallest hydrated oxalate cluster observed was $C_2O_4^{2-}(H_2O)_3$. Two hydrated hydroxide clusters, $OH^-(H_2O)_n$ ($n=1,2$), were also observed (the $n=2$ species is labeled in Fig. 1). The mass-to-charge (m/z) ratios of $OH^-(H_2O)_m$, $m=3$, 4, 5,..., are the same as those of the $C_2O_4^{2-}(H_2O)_n$ clusters with odd number of water, $n=3$, 5, 7,..., respectively, and could not be distinguished in the mass spectrum. However, the intensity of the hydroxide clusters was observed to decrease rapidly with the number of water. As will be shown below, the $OH^-(H_2O)_m$ and $C_2O_4^{2-}(H_2O)_n$ clusters have very different electron binding energies and can be easily distinguished in the PES spectra. The PES spectra of $C_2O_4^{2-}(H_2O)_n$ indicated no hydroxide cluster contamination for $n \geqslant 7$, suggesting that the mass intensities of $OH^-(H_2O)_m$ ($m \geqslant 5$) were negligible. The mass spectrum tentatively suggested that $C_2O_4^{2-}$ needs at least three H_2O molecules to be stabilized in the gas phase.

B. Photoelectron spectra of $C_2O_4^{2-}(H_2O)_3$

Figure 2 shows the PES spectra of $C_2O_4^{2-}(H_2O)_3$ at 266 and 193 nm. The 193 nm spectrum was dominated by two bands at high binding energies, which were from detachment

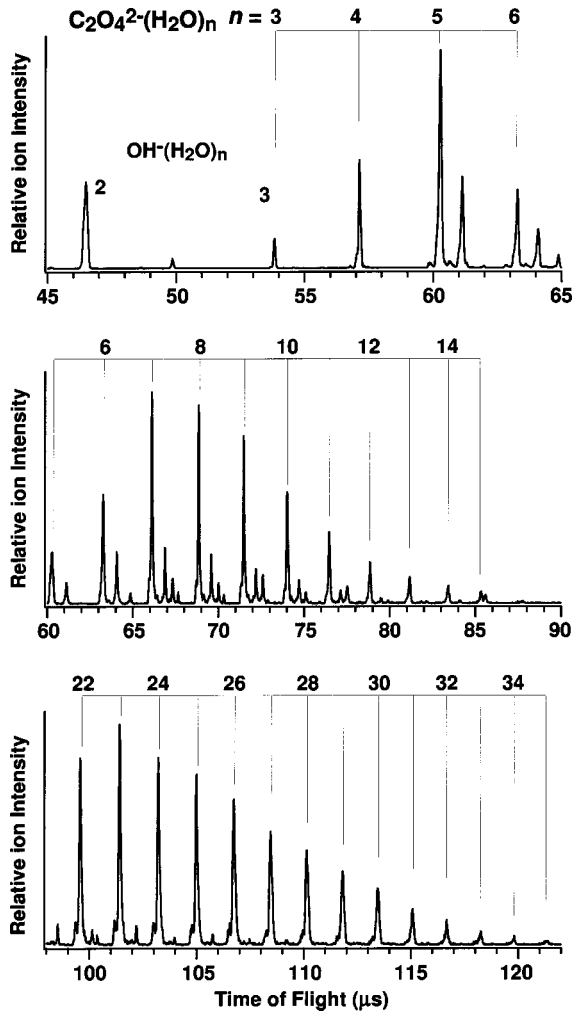

FIG. 1. A typical mass spectrum, optimized for three mass ranges, of $C_2O_4^{2-}(H_2O)_n$ from electrospray ionization of a potassium oxalate solution.

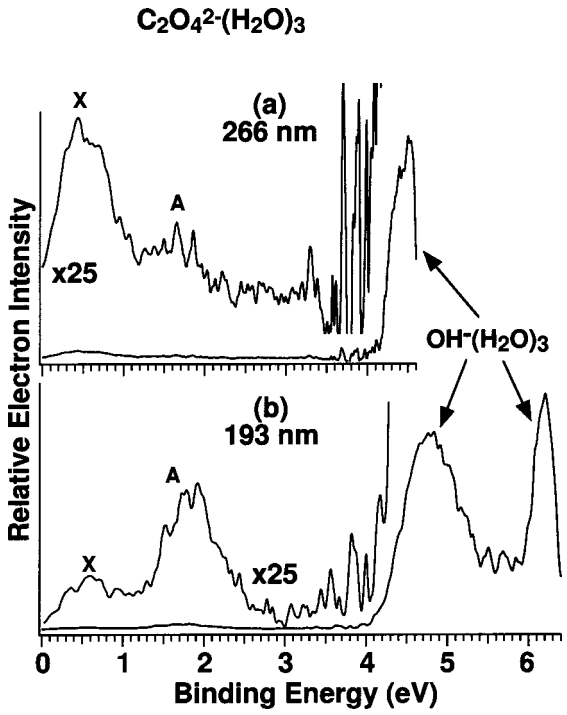

FIG. 2. Photoelectron spectra of $C_2O_4^{2-}(H_2O)_3$ at (a) 266 nm and (b) 193 nm. Note the dominant signals of $OH^-(H_2O)_3$, which has an identical m/z ($=71$) as $C_2O_4^{2-}(H_2O)_3$.

of $OH^-(H_2O)_3$.[45] Weak signals, due to $C_2O_4^{2-}(H_2O)_3$, were present at the lower binding energy side. As we have shown previously,[46–49] multiply-charged anions universally possess a repulsive coulomb barrier (RCB), which prevents photoemission of low kinetic energy electrons. Because the RCB cut off transitions on the high binding energy side for $C_2O_4^{2-}(H_2O)_3$, the spectra of the hydrated hydroxide and oxalate in fact did not overlap. The weak photoemission signals for $C_2O_4^{2-}(H_2O)_3$ suggested that the $m/z=71$ peak in the mass spectrum (Fig. 1) was primarily from $OH^-(H_2O)_3$. The two features (X and A) from the hydrated oxalate were similar to those of the large solvated oxalate clusters (Figs. 3 and 4). The ADE and VDE of $C_2O_4^{2-}(H_2O)_3$ were estimated to be 0.0 ± 0.1 and 0.5 ± 0.1 eV, respectively. Therefore, $C_2O_4^{2-}(H_2O)_3$ is barely stable and may even be slightly unstable, considering the uncertainty. Thus, at least three waters are needed to stabilize $C_2O_4^{2-}$ in the gas phase.

C. Photoelectron spectra of $C_2O_4^{2-}(H_2O)_n$ ($n=4-40$)

The PES spectra of $C_2O_4^{2-}(H_2O)_n$ were taken at several photon energies, 157 nm ($n=4-40$), 193 nm ($n=3-25$), and 266 nm ($n=3-14$). For the large clusters ($n\geqslant25$), only 157-nm spectra were measured, due to their electron high binding energies. Figure 3 shows the PES spectra of $C_2O_4^{2-}(H_2O)_n$ ($n=4-40$) at 157 nm. In the size range from $n=4$ to 20, only clusters with an even number of solvent were presented. The smaller cluster with odd number of solvent contained contributions from hydrated hydroxide and were not shown here. For $n>20$, only four spectra were taken at an interval of five because the spectral changes were very gradual as a function of n.

Several observations can be made about the data in Fig. 3. First, the ADE, which measures the electronic stability of $C_2O_4^{2-}(H_2O)_n$, increases steadily with the number of water, from ~0.5 eV ($n=4$) to ~4.7 eV ($n=40$). Second, the spectral patterns of the hydrated oxalate are all very similar and appear to shift rigidly to higher binding energies as a function of solvent number. Third, the intensities of the first two features decreased gradually with increasing solvation, and became very weak for $n>20$, whereas the band at the high binding energy side increased and became dominant for the larger clusters. Fourth, all the spectra seemed to be cut off at the high binding energy side, due to the RCB,[46–49] which will be discussed later. In the spectra of the larger clusters ($n>10$), the RCB appeared to cut off the third band, giving rise to the appearance of a sharp peak. Finally, the first two features of the spectra of $C_2O_4^{2-}(H_2O)_n$ are all similar to that of $K^+[C_2O_4^{2-}]$ (Fig. 4), suggesting that the two PES features are from intact $C_2O_4^{2-}$ in the hydrated clusters. There exists a third peak (B) in the $K^+[C_2O_4^{2-}]$ spectrum (Fig. 4), but it is too weak to account for the third broad band in the spectra of $C_2O_4^{2-}(H_2O)_n$ (Fig. 3). Thus the third band in the hydrated clusters was mainly due to another ionization channel—direct ionization of water (Sec. VI C).

The photon-energy-dependent PES spectra of

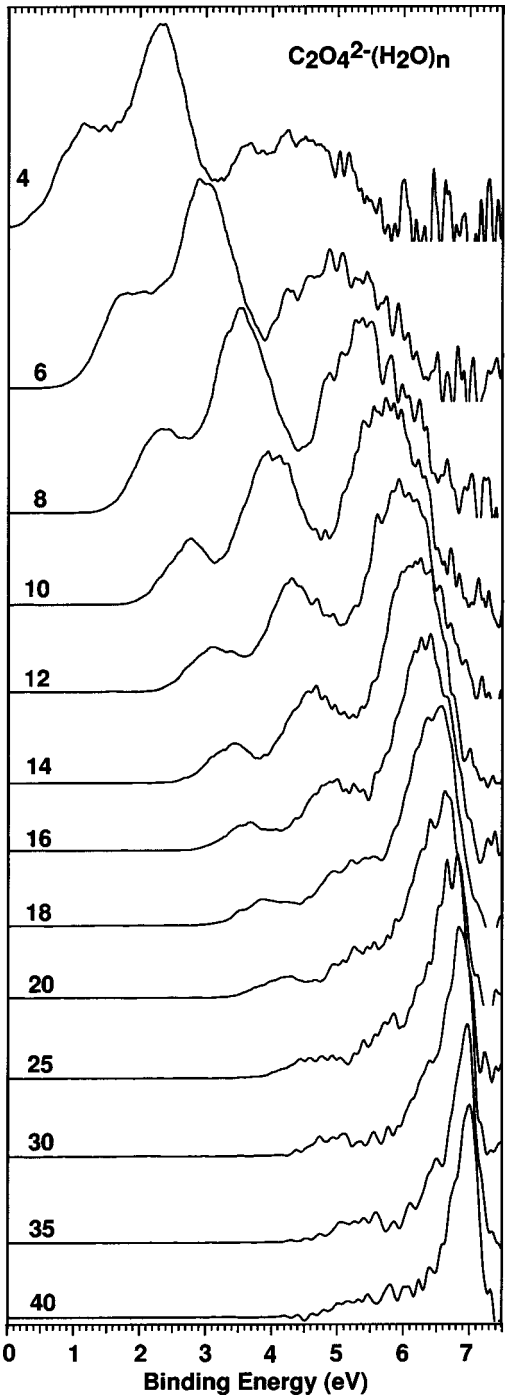

FIG. 3. Overview of the photoelectron spectra of $C_2O_4^{2-}(H_2O)_n$ ($n=4-40$) at 157 nm.

$C_2O_4^{2-}(H_2O)_n$ ($n=4,6,8,10,12$) are shown in Figs. 5–9, respectively, showing the disappearance of the high binding energy features in the lower photon energy spectra, as a direct consequence of the RCB in multiply-charged anions. From these data the barrier height for each dianion can be estimated, as discussed in Sec. VI A. The first peak in the 266-nm spectra of $C_2O_4^{2-}(H_2O)_n$ ($n=4-12$) appeared to shift gradually to low binding energies relative to that in 193 nm, as indicated by the vertical line. The PES signals at 266 nm decreased as n increased, and there were no detectable electron signals for $n>16$. As will be discussed below, both

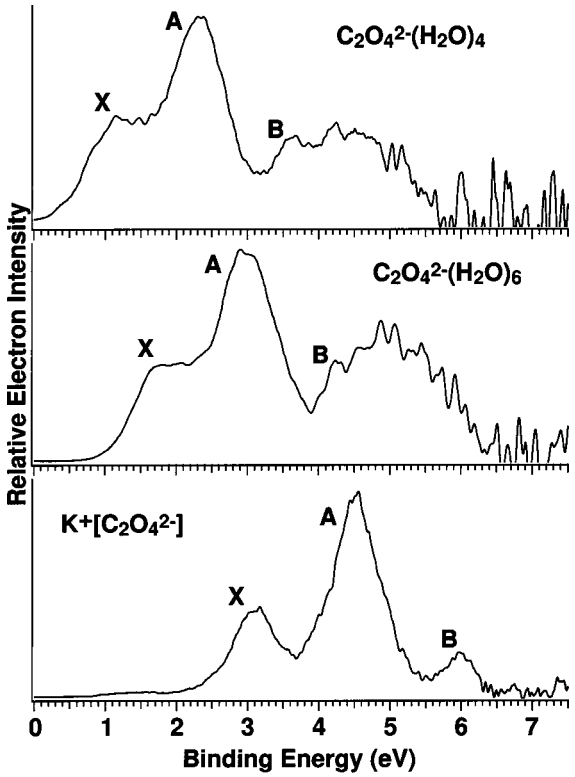

FIG. 4. 157-nm photoelectron spectra of $C_2O_4^{2-}(H_2O)_n$ ($n=4$ and 6) compared to that of $K^+[C_2O_4^{2-}]$.

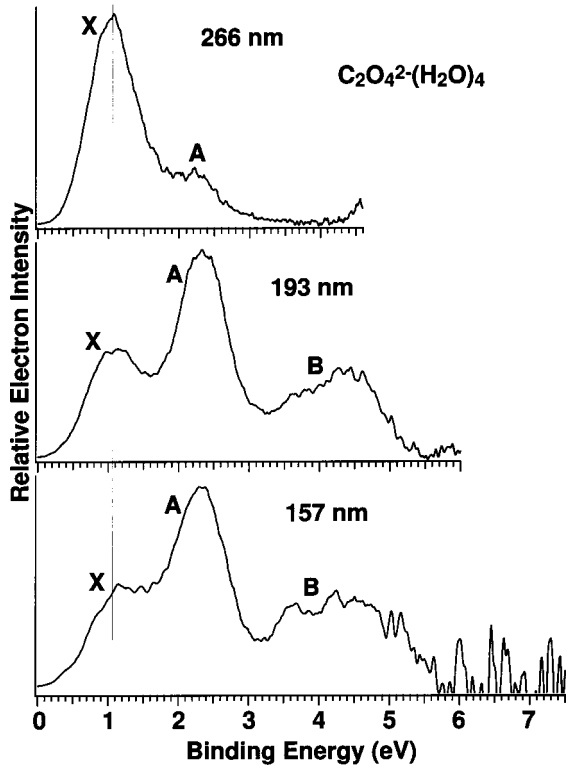

FIG. 5. Photoelectron spectra of $C_2O_4^{2-}(H_2O)_4$ at 266, 193, and 157 nm.

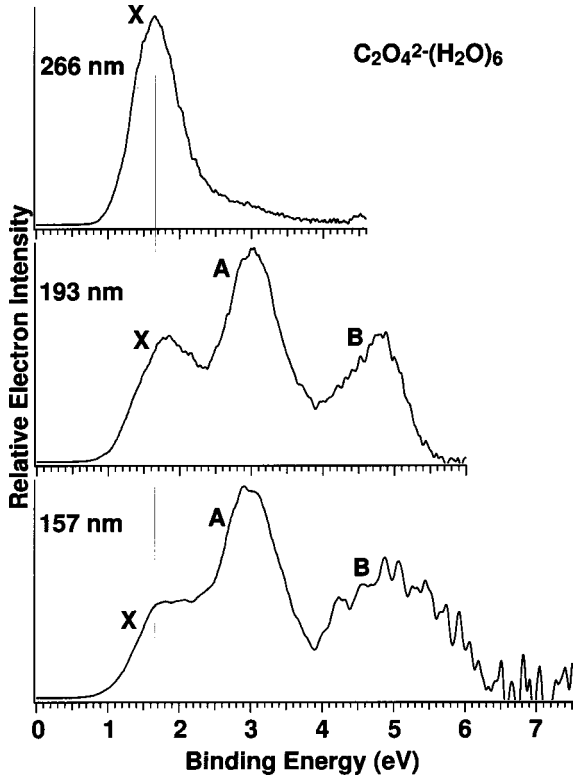

FIG. 6. Photoelectron spectra of $C_2O_4^{2-}(H_2O)_6$ at 266, 193, and 157 nm.

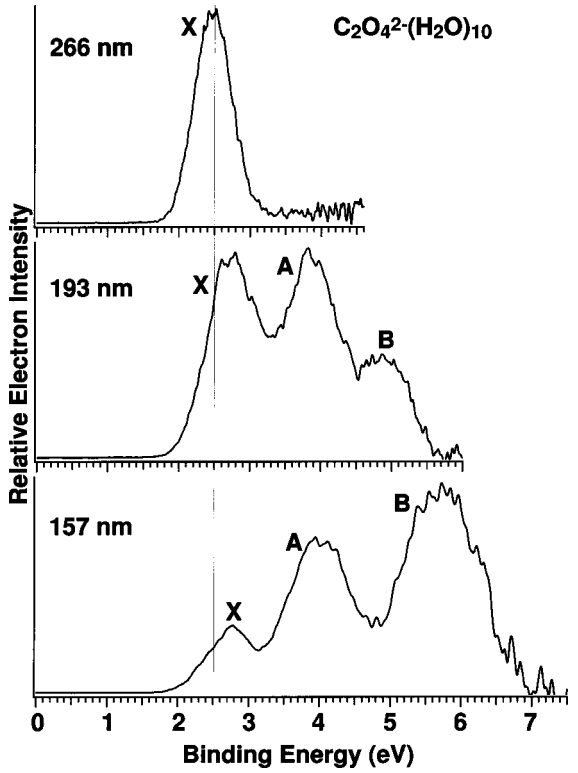

FIG. 8. Photoelectron spectra of $C_2O_4^{2-}(H_2O)_{10}$ at 266, 193, and 157 nm.

of these observations were directly due to the presence of the RCB.[48]

The adiabatic detachment energy (ADE) was estimated by drawing a straight line at the leading edge of the ground state transition and then adding a constant to the intercept with the binding energy axis to take into account of the instrumental resolution, ranging from 0.03 to 0. 1 eV depending on the electron kinetic energies. This procedure was

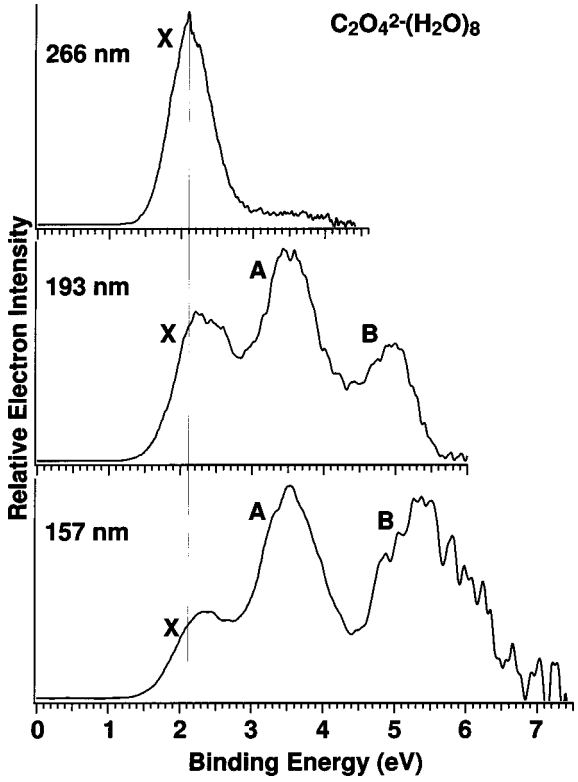

FIG. 7. Photoelectron spectra of $C_2O_4^{2-}(H_2O)_8$ at 266, 193, and 157 nm.

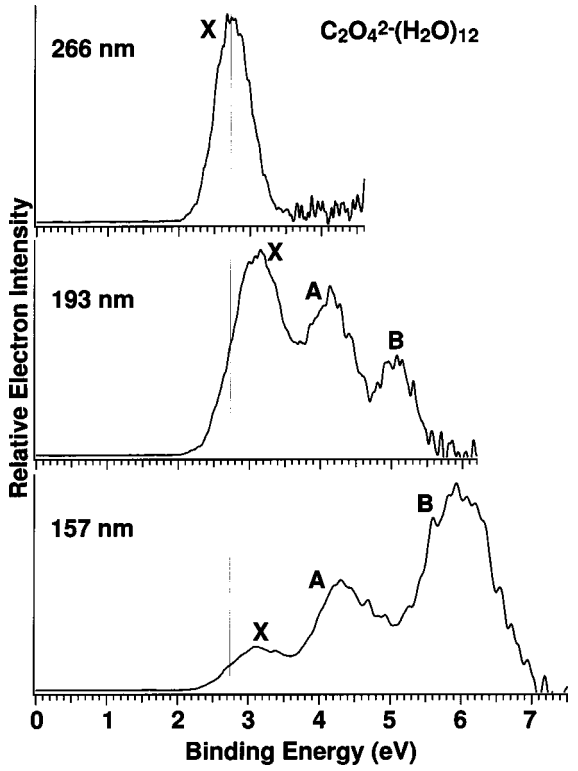

FIG. 9. Photoelectron spectra of $C_2O_4^{2-}(H_2O)_{12}$ at 266, 193, and 157 nm.

TABLE I. Adiabatic detachment energies (ADE) of $C_2O_4^{2-}$ and H_2O, and vertical detachment energies (VDE) of $C_2O_4^{2-}$ in the hydrated clusters, $C_2O_4^{2-}(H_2O)_n$. The calculated ADE for $n=0-6$ are shown for comparison. All energies are in eV.[a]

	Expt. ($C_2O_4^{2-}$)				Theor. ($C_2O_4^{2-}$)		H_2O (ADE)
n	ADE	ΔADE[b]	VDE	ΔVDE[b]	VDE	ΔVDE[b]	
0					−1.63		
1					−0.89	0.74	
2					−0.13	0.76	
3	0.00		0.50		0.48	0.61	
4	0.51	0.51	1.14	0.64	1.06	0.58	
5	0.85	0.34	1.43	0.29	1.44	0.38	
6	1.17	0.32	1.84	0.41	1.75	0.31	
7	1.48	0.31	2.05	0.21			
8	1.74	0.26	2.32	0.27			
9	1.96	0.22	2.55	0.23			
10	2.18	0.22	2.75	0.20			4.87
12	2.53	3.11					5.20
14	2.84	3.41					5.42
16	3.10	3.65					5.50
18	3.35	3.88					5.65
20	3.54	4.17					5.70
25	3.96	4.58					6.04
30	4.40	4.94					6.16
35	4.67	5.32					6.32
40	4.76	5.46					6.54

[a]Experimental uncertainty: ±0.10 eV.
[b]$\Delta\mathrm{ADE}(n)=\mathrm{ADE}(n)-\mathrm{ADE}(n-1)$; $\Delta\mathrm{VDE}(n)=\mathrm{VDE}(n)-\mathrm{VDE}(n-1)$.

rather approximate, which is reflected in the large uncertainties given for the derived ADEs. The vertical detachment energy (VDE) was determined from the peak maximum. The obtained ADEs and VDEs are listed in Table I and shown in Fig. 10.

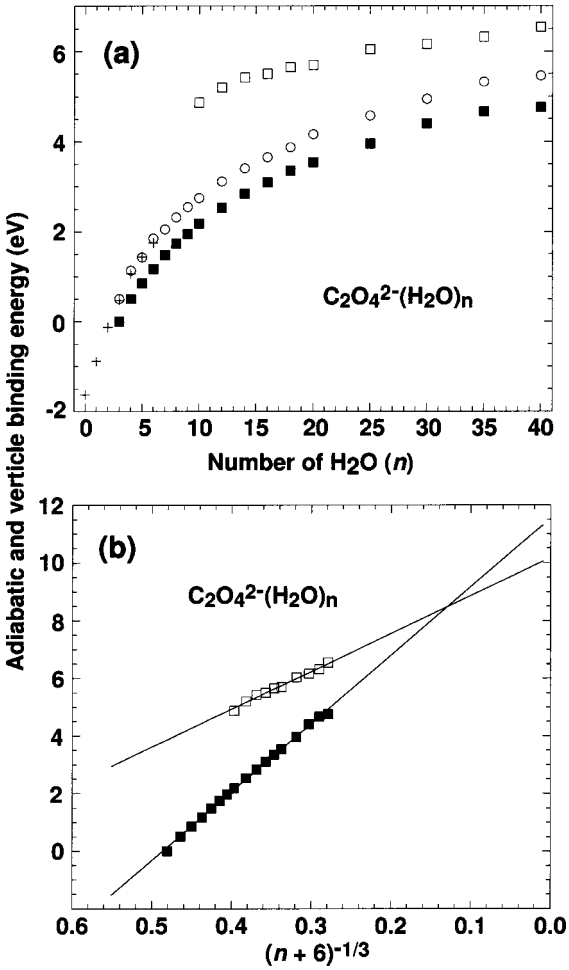

FIG. 10. (a) Experimental adiabatic (filled squares) and vertical (open circles) electron binding energies of $C_2O_4^{2-}(H_2O)_n$ ($n=3-40$), along with the calculated VDEs for $n=0-6$ (crosses) as a function of n. The ionization thresholds of water are also shown (open squares). (b) ADEs of $C_2O_4^{2-}$ (filled squares) and H_2O (open squares) in $C_2O_4^{2-}(H_2O)_n$ as a function of $(n+6)^{-1/3}$ (proportional to 1/cluster-radius).

V. THEORETICAL RESULTS

The minimum energy structures of $C_2O_4^{2-}(H_2O)_n$ are shown in Fig. 11 ($n=0-4$) and Fig. 12 ($n=5,6$) with the bond lengths and angles indicated. The optimized structure of $C_2O_4^{2-}$ has D_{2d} symmetry, consistent with a recent theoretical study.[38] For the clusters with $n=1-4$, each of the water molecules are strongly bound to the $C_2O_4^{2-}$ core via two H-bonds without interwater H-bonding, similar to the hydration of sulfate.[35] For the two clusters with $n=5$ and 6, however, water–water H-bonding appears. The fifth water forms one H-bond with oxalate and another H-bond with a neighboring water, which now forms only one H-bond with the ion core instead. The sixth H_2O interacts with $C_2O_4^{2-}$ via one H-bond, so that one of the O of the oxalate dianion has three H-bonds in $C_2O_4^{2-}(H_2O)_6$.

The calculated VDEs corresponding to these structures are in excellent agreement with the experimental data (Table I and Fig. 10), lending considerable credence for the validity of these structures. The theoretical results confirmed that indeed $C_2O_4^{2-}(H_2O)_n$ with $n=0-2$ are electronically unstable: the calculated VDEs are −1.63, −0.89, and −0.13 eV, respectively. The calculations also confirmed that $C_2O_4^{2-}$ exists as a distinct structural unit with minimal perturbations in all the solvated clusters; the C–C and C–O bond lengths differ only slightly from the free $C_2O_4^{2-}$ structure.

VI. DISCUSSIONS

A. Photon-energy-dependent studies, the RCB, and intramolecular Coulomb repulsion

One unique property of multiply-charged anions is the existence of the intramolecular Coulomb repulsion between the excess charges.[46–49] When an electron is removed from a multiply-charged anion (A^{n-}), the two photoproducts ($A^{(n-1)-}+e^-$) are both negatively charged. The superposition of the long-range Coulomb repulsion between the outgoing electron and the remaining anion and the short-range electron binding produces an effective potential barrier for the outgoing electron. A similar potential barrier exists for dications relative to dissociation.[50] The Coulomb repulsion and the resulting RCB have profound effects on the chemical and physical properties of multiply-charged anions.[46–49] We have shown that the Coulomb repulsion is equal in magni-

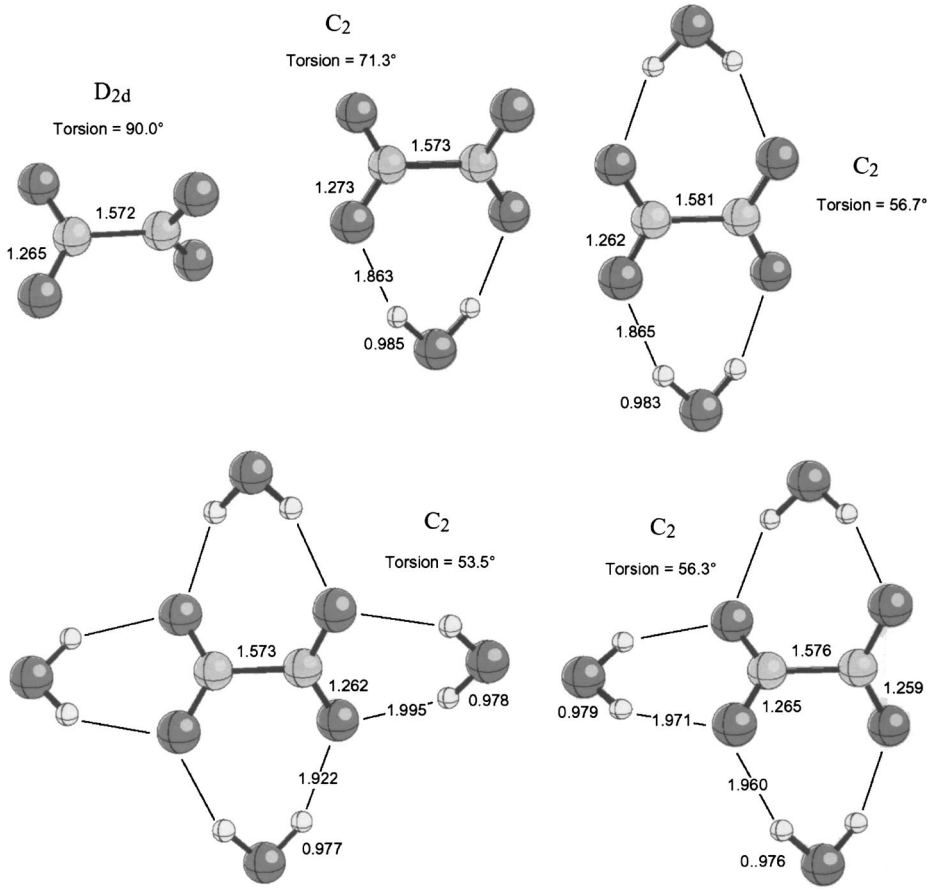

FIG. 11. Optimized structures for the lowest energy isomers of $C_2O_4^{2-}(H_2O)_n$ $(n=0-4)$ at the B3LYP/TZVP+ level. Selected bond lengths are given in Å.

tude to the RCB if the detached electron is localized on the charge carrier group.[49] In general, the RCB decreases with increasing physical sizes of multiply-charged anions.

We have taken the PES spectra of $C_2O_4^{2-}(H_2O)_n$ $(n=3-25)$ at several different photon energies (i.e., Figs. 5–9 for $n=4-12$), from which the height of the RCB can be estimated. The RCB effects on the PES data were seen most clearly in the photon-energy-dependent PES spectra, where the high binding energy features observed at high photon energies were severely cut off in the low photon energy spectra (Figs. 5–9). On the basis of the spectral cut-off, the magnitude of the RCB could be estimated by subtracting the binding energies at the cut-off point from the photon energies. Here we use the spectra of $C_2O_4^{2-}(H_2O)_6$ as an example (Fig. 6). The disappearance of feature-A in the 266-nm spectrum indicates that the 266-nm photon energy (4.661 eV) lies below the top of the RCB corresponding to this detachment channel. Thus the RCB has to be larger than 1.6 eV ($h\nu$- VDE of the *A* state, i.e., 4.6–3.0 eV). The strong *A* feature at 193 nm suggests the RCB$<$3.4 eV (6.4–3.0 eV). The relatively strong and slightly shifted *X* peak at 1.6 eV in the 266-nm spectrum implies that the RCB must be close to 3.0 eV (4.6 eV–1.6 eV). Therefore the RCB of $C_2O_4^{2-}(H_2O)_6$ is estimated to be $\sim$3.0 eV. Similarly we es-

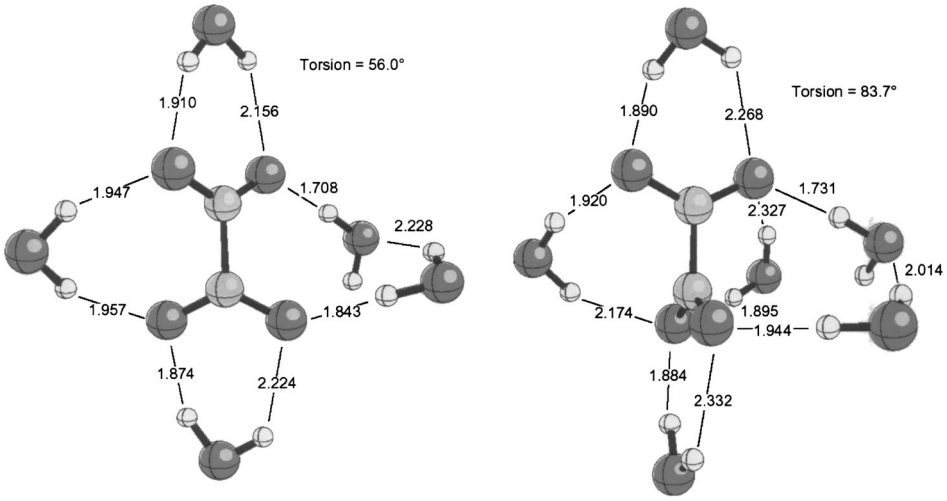

FIG. 12. Optimized structures for the lowest energy isomers of $C_2O_4^{2-}(H_2O)_n$ $(n=5$ and 6) at the B3LYP/TZVP+ level. Selected bond lengths are given in Å.

TABLE II. Estimated repulsive Coulomb barrier for $C_2O_4^{2-}(H_2O)_n$ in eV.[a]

n	0[b]	3	4	5	6	7	8	9	10	12	14	16	18	20	25
	4.6	3.5	3.3	3.1	3.0	2.7	2.5	2.4	2.3	2.2	2.0	2.0	2.0	1.9	1.9

[a]Uncertainty: ± 0.1 eV.

[b]RCB of free $C_2O_4^{2-}$ was estimated from a simple point-charge approximation, assuming two charges are localized on the two oxygen atoms of each $-CO_2$ group. The charge separation was calculated from the optimized structure (Fig. 11).

timated the RCBs for all $C_2O_4^{2-}(H_2O)_n$ from the photon-energy-dependent PES spectra, as given in Table II. The estimated RCBs decrease with increasing solvation, from ~ 3.5 eV ($n=3$) to ~ 1.9 eV ($n=25$).

B. The minimum number of H_2O required to stabilize $C_2O_4^{2-}$ in the gas phase

The two excess charges in $C_2O_4^{2-}$ should be distributed over the four oxygen atoms. Using the optimized structure of free $C_2O_4^{2-}$ (Fig. 11), we can estimate its intramolecular Coulomb repulsion. Using the diagonal O–O distance (3.15 Å), we obtain a Coulomb repulsion energy of ~ 4.6 eV ($e^2/4\pi\varepsilon_0 r = 14.4/r$ in eV, where r in Å). Our estimated intramolecular Coulomb repulsion in $C_2O_4^{2-}(H_2O)_3$ is ~ 3.5 eV (Table II). The first three waters thus reduce the intramolecular Coulomb repulsion in $C_2O_4^{2-}$ by more than 1 eV, which is sufficient to stabilize $C_2O_4^{2-}$ in the gas phase.

Herbert and Ortiz recently carried out *ab initio* calculation on the free $C_2O_4^{2-}$.[38] They predicted its ADE and VDE to be -2.1, and -1.28 eV at the MP2//6-311+++G* level, which agrees with our calculated VDE of -1.63 eV. Our calculated VDEs for $C_2O_4^{2-}(H_2O)_n$ are -0.89, -0.13, and 0.48 eV for $n=1-3$, respectively (Table I), suggesting one or even two water molecules are not sufficient to stabilize $C_2O_4^{2-}$ in the gas phase. We measured an ADE of 0.0 eV for $C_2O_4^{2-}(H_2O)_3$, meaning that three waters are barely enough to stabilize $C_2O_4^{2-}$, consistent with the theoretical predictions. The PES results provide the most conclusive evidence that *three* is the minimum number of H_2O needed to stabilize $C_2O_4^{2-}$ in the gas phase. Previously we have shown that SO_4^{2-} also requires three waters to be stabilized as a gaseous species.[35]

C. Assignments of the spectral features: Detachment from $C_2O_4^{2-}$ and ionization of water

Figure 3 shows that the first two PES features of the hydrated oxalate clusters are all very similar, except that their relative intensities seemed to decrease with increasing degree of solvation. These two features exhibited the same pattern compared to that of $KC_2O_4^-$ (Fig. 4), indicating that they were due to detachment from the solute $C_2O_4^{2-}$. Thus we can conclude that $C_2O_4^{2-}$ remained intact in the hydrated clusters and there was no proton transfer reactions, such as $C_2O_4^{2-}(H_2O)_n \rightarrow HC_2O_4^-(H_2O)_{n-1}(OH^-)$. Our calculations also indicate that $C_2O_4^{2-}$ is largely unperturbed in the solvated clusters (Fig. 11).

However, what is the nature of the intense high binding energy feature in $C_2O_4^{2-}(H_2O)_n$? This feature was relatively weak, but broad for smaller clusters and gained intensity with increasing n, becoming dominant for $n>10$. Similar to the two $C_2O_4^{2-}$ features, this band also shifted to high binding energies with increasing n and began to be cut off by the RCB for $n>10$ (Fig. 3). This feature could not be accounted for by the relatively weak contribution of the third peak from $C_2O_4^{2-}$ (feature B in Fig. 4). As we showed previously,[36] this intense high binding energy feature corresponds to a new detachment channel: the ionization of the solvent. The ionization potentials of water clusters should be between that of gaseous water molecules at 12.6 eV and that of liquid water at 10.06 eV.[29] However, because the solvated clusters were negatively charged, the ionization potentials of water were greatly lowered. For example, we have observed that the ionization potential of a water molecule was reduced from 12.6 to about 6.1 eV in the F^-H_2O complex,[51] because of the strong Coulomb repulsion experienced by the valence electrons in H_2O from F^-. We also observed that the intensity of the solvent ionization peak increased rapidly with the solvent number.[51] For $C_2O_4^{2-}(H_2O)_n$ clusters, the ionization of water was present even in the small clusters starting at $n=4$ in the 157 nm spectra. The decrease of the RCB and the enhanced ionization cross section with increasing solvent numbers made the photoemission signals from the solvent become the dominant PES feature in the large clusters of $C_2O_4^{2-}(H_2O)_n$.

Therefore, the onset of the intense high binding energy peak represented the ionization potentials of water in the $C_2O_4^{2-}(H_2O)_n$ solvated clusters. This value was estimated from the PES spectra, as given in Table I for $n=10-40$ and plotted in Fig. 10. The overlap between the B band of the solute (Fig. 4) and the band from water prevented us from obtaining the solvent ionization thresholds for the smaller systems.

D. Stepwise hydration of oxalate in $C_2O_4^{2-}(H_2O)_n$ ($n=0-6$)

Although PES cannot directly yield information about the geometric structures of the solvated clusters, the electron binding energy revealed from the spectra is sensitive to the solvation environment. The ADEs and VDEs of $C_2O_4^{2-}(H_2O)_n$ ($n=3-40$) increase systematically with the number of H_2O (Table I and Fig. 10). The stabilization derives from charge-dipole interactions and reduction of the intramolecular Coulomb repulsion. Our theoretical calculations show that the first two waters have the strongest stabilization effect, each stabilizing oxalate by ~ 0.75 eV (Table I). The differential stabilization energy decreases to ~ 0.6 eV for $n=3$ and 4 and further drops to ~ 0.38 and 0.31 eV for $n=5$ and 6. For the larger clusters, the differential stabiliza-

tion energy (ΔADE) gradually decreases. Thus, the first four waters have the strongest stabilization effect on $C_2O_4^{2-}$.

A clear stepwise picture of how $C_2O_4^{2-}$ is solvated by H_2O molecules emerges from the calculated structures, shown in Figs. 11 and 12. The first water molecule strongly interacts with the oxalate, forming two H-bonds with two oxygen atoms from the two carboxylates and reducing the torsion angle to 71.3°. The second water bonds similarly to the other two O atoms, further reducing the torsion angle between the two carboxylates to 56.7°, compared to 90° in free $C_2O_4^{2-}$. The first two waters have the strongest stabilizing effect on oxalate because each H from the waters is able to H-bond to one O atom from $C_2O_4^{2-}$. The third and fourth water molecules also interact with oxalate via two H-bonds, each on one end of the $-CO_2^-$ group. However, the two O atoms that the third and fourth water bridges already interact with the first two H_2O and thus the stabilization energy is slightly lowered.

How do the fifth and sixth H_2O solvate the oxalate after the strong screening of the two negative charges by the first four H_2O? Our geometry optimization shows that the fifth water forms only a single H-bond with oxalate and another H-bond with one of the first two waters bridging the two carboxylate ends, leaving only one H-bond for this water with the ion core. The sixth H_2O again singly H-bonds to the oxalate on the same side of the water dimer in $C_2O_4^{2-}(H_2O)_5$, forming a water trimer on one side of the solvated cluster. The differential stabilization energies of the fifth and sixth H_2O are further lowered. Hence the tetrahydrated oxalate is special, in which each O atom on the oxalate are forming two H-bond with the solvent. Further hydration leads to water–water H-bonding.

E. Interior versus surface solvation

The most surprising finding was the decrease of the $C_2O_4^{2-}$ photoemission features and the increase of the solvent feature with increasing degree of solvation in the 157-nm PES spectra of $C_2O_4^{2-}(H_2O)_n$ ($n=3-40$) (Fig. 3). In fact, the $C_2O_4^{2-}$ features almost completely disappeared and the high binding energy peak due to photoemission from water became the only feature in clusters with $n>20$. Previously we have observed the same phenomenon in hydrated SO_4^{2-} clusters and interpreted the observation as due to the fact that the solute is solvated in the center of the solvated clusters.[36] This is distinctly different from the surface-hydrated I^- clusters, $I^-(H_2O)_n$, whose photoemission features from the solute I^- were observed for n as large as 60.[20] Our *ab initio* calculations for up to six waters showed that indeed the water molecules tend to solvate symmetrically around $C_2O_4^{2-}$ (Figs. 11 and 12).

Therefore, the decrease of the $C_2O_4^{2-}$ photoemission suggested that the oxalate dianion should be solvated in the center of the water clusters so that the electron signals from the oxalate were suppressed by the solvation layer. This interpretation is supported by a previous photoemission study at 21.2 eV of a highly concentrated aqueous solution of CsF.[27] In this experiment, photoemission from F^- was significantly reduced by a one-layer water solvation shell on F^- at the solution–vacuum interface.[52] Furthermore, a small mixture of CsI into the CsF solution showed that photoemission features from I^- were actually enhanced because I^- was more surface-active. These observations in the bulk electrolyte solutions were consistent with the observations in the gas-phase solvated clusters, where I^- is known to be solvated on the outside of the water clusters[16] and F^- on the inside due to its strong charge-dipole interactions with water.[16,19]

F. Transition from molecularlike clusters to bulk aqueous solution

Previous theoretical considerations of ion solvation in finite clusters suggested that the ionization energies of a solvated anion should be scaled to $1/R$ linearly,[53,54] where R is the radius of the solvated clusters and is proportional to the solvent number as $(n+\delta)^{-1/3}$ (δ is the equivalent solvent number for the solute and accounts for the contribution of the solute to the cluster volume). For example, in $I^-(H_2O)_n$, δ has been taken to be 2 for I^-.[20] We estimated that δ is 6 for $C_2O_4^{2-}$ and 4 for SO_4^{2-}.[36] In Fig. 10(b), we plot the ionization thresholds for the solutes and solvent as a function of $(n+\delta)^{-1/3}$. The ionization thresholds for the solutes as well as that for water were indeed linearly dependent on $(n+\delta)^{-1/3}$. Importantly, the ionization energies for water extrapolated to 10.2 eV for the $C_2O_4^{2-}(H_2O)_n$ system, for infinitive n, and are consistent with the threshold ionization energy of bulk water at 10.06 eV.[29] This observation lent considerable credence for the assignment of the high binding energy feature to ionization of water in the solvated systems because for an infinitively large water cluster the central anion should have negligible effect to the ionization energy of the water cluster. However, the ionization energy of $C_2O_4^{2-}$ was extrapolated to a very large value, 11.5 eV, in an infinitively large $C_2O_4^{2-}(H_2O)_n$ cluster. This value differs from the ionization threshold of oxalate estimated for bulk oxalate aqueous solution, 7.32 eV.[29] We attribute this discrepancy to the fact that the bulk value was measured over the surface of an oxalate electrolyte solution at a relatively high solute concentration (1 M), whereas our extrapolation corresponded to a hypothetical situation in which a single solute is solvated in the center of an infinitely large water cluster, i.e., an infinitely dilute solution.

The dimensions of our largest solvated clusters were greater than 1 nm and they can be viewed as nanowater droplets doped with a single oxalate dianion. We observed that these nanosized aqueous clusters began to exhibit electronic properties similar to bulk electrolyte solutions. A smooth transition from solvated oxalate clusters to behaviors of an oxalate solution was thus observed one solvent molecule at a time. Although photoemission from oxalate dominated in small clusters, photoelectrons from the solutes were trapped by the solvent in the large clusters, producing ''solvated'' electrons (instead of electron emission to vacuum), analogous to the generation of solvated electrons in bulk aqueous solutions.[55] The ionization of the solvent, however, would produce a ''hole,'' that could react with the solutes through charge migration or react with a neighboring water molecule to generate $OH+H_3O^+$, a process known to occur

in bulk solutions.[55] These photophysical processes taking place in the solvated clusters may be investigated using pump–probe experiments.[23,56,57] Therefore, in addition to being as structural models, the nanosolvated clusters may be used as molecular analogs for the investigation of a variety of properties of aqueous electrolyte solutions.

VII. CONCLUSIONS

We report a photoelectron spectroscopic and theoretical study of hydrated oxalate dianions. We found that a free gaseous $C_2O_4^{2-}$ dianion needs at least three waters to be stabilized. Our calculations show that the first four waters bind tightly to $C_2O_4^{2-}$, each forming two H-bonds with $C_2O_4^{2-}$ without interwater H-bonding. Photoemission features from both the solute and the solvents were observed and were distinguished by comparing with the spectrum of an oxalate ion pair ($K^+C_2O_4^{2-}$). The binding energies of the solute photoemission features increase systematically with increasing solvation. Photon-energy-dependent studies allowed us to estimate the RCB and the intramolecular Coulomb repulsion, which was shown to decrease as a function of n. The relative intensities of the solute photoemission features gradually diminished as water coverage increased, whereas the solvent ionization feature grew in intensity and became dominant for larger n. This observation suggested that $C_2O_4^{2-}$ is solvated in the center of the water clusters so that electrons detached from the solute were suppressed by the surrounding solvent, similar to photoemission of bulk aqueous solutions.

ACKNOWLEDGMENTS

This work was supported by The U.S. Department of Energy, Office of Basic Energy Sciences, Chemical Science Division and partly by The Petroleum Research Fund, administered by the American Chemical Society. The work was performed at the EMSL, a national scientific user facility sponsored by DOE's Office of Biological and Environmental Research and located at Pacific Northwest National Laboratory, operated for DOE by Battelle.

[1] N. Nandi, K. Bhattacharyya, and B. Bagchi, Chem. Rev. **100**, 2013 (2000).
[2] H. Ohtaki and T. Radnai, Chem. Rev. **93**, 1157 (1993).
[3] Y. Marcus, Chem. Rev. **88**, 1475 (1988).
[4] M. R. Waterland, D. Stockwell, and A. M. Kelley, J. Chem. Phys. **114**, 6249 (2001).
[5] A. Pasquarello, I. Petri, P. S. Salmon, O. Parisel, R. Car, É. Tóth, D. H. Powell, H. E. Fischer, L. Helm, and A. E. Merbach, Science **291**, 856 (2001).
[6] M. F. Kropman and H. J. Bakker, Science **291**, 2118 (2001).
[7] M. Klein, Science **291**, 2106 (2001); D. A. Yarne, M. E. Tuckerman, and M. L. Klein, Chem. Phys. **258**, 163 (2000).
[8] W. R. Cannon, B. M. Pettitt, and J. A. McCammon, J. Phys. Chem. **98**, 6225 (1994).
[9] E. V. Stefanovich, A. I. Boldyrev, T. N. Truong, and J. Simons, J. Phys. Chem. B **102**, 4205 (1998).
[10] L. X. Dang and T.-M. Chang, J. Phys. Chem. B **106**, 235 (2002).
[11] P. B. Balbuena, K. P. Johnston, and P. J. Rossky, J. Phys. Chem. **100**, 2706 (1996).
[12] G. Niedner-Schatteburg and V. E. Bondybey, Chem. Rev. **100**, 4059 (2000).
[13] J. V. Coe, A. D. Earhart, M. H. Cohen, G. J. Hoffman, H. W. Sarkas, and K. H. Bowen, J. Chem. Phys. **107**, 6023 (1997).
[14] J. V. Coe, J. Phys. Chem. A **101**, 2055 (1997).
[15] S. S. Xantheas, J. Phys. Chem. **100**, 9703 (1996); J. Am. Chem. Soc. **117**, 10373 (1995).
[16] L. Perera and M. L. Berkowitz, J. Chem. Phys. **100**, 3085 (1994); **99**, 4222 (1993); **96**, 8288 (1992).
[17] W. H. Thompson and J. T. Hynes, J. Am. Chem. Soc. **122**, 6278 (2000).
[18] I. A. Topol, G. J. Tawa, S. K. Burt, and A. A. Rashin, J. Chem. Phys. **111**, 10998 (1999).
[19] O. M. Cabarcos, C. J. Weinheimer, J. M. Lisy, and S. S. Xantheas, J. Chem. Phys. **110**, 5 (1999).
[20] G. Markovich, S. Pollack, R. Giniger, and O. Cheshnovsky, J. Chem. Phys. **101**, 9344 (1994).
[21] P. Ayotte, G. H. Weddle, and M. A. Johnson, J. Chem. Phys. **110**, 7129 (1999).
[22] J. H. Choi, K. T. Kuwata, Y. B. Cao, and M. Okumura, J. Phys. Chem. A **102**, 503 (1998).
[23] L. Lehr, M. T. Zanni, C. Frischkorn, R. Weinkauf, and D. M. Neumark, Science **284**, 635 (1999).
[24] B. J. Greenblatt, M. T. Zanni, and D. M. Neumark, Science **276**, 1675 (1997).
[25] J. M. Weber, J. A. Kelley, S. B. Nièlsen, P. Ayotte, and M. A. Johnson, Science **287**, 2461 (2000); J. M. Weber, J. A. Kelley, W. H. Robertson, and M. A. Johnson, J. Chem. Phys. **114**, 2698 (2001).
[26] H. Siegbahn, J. Phys. Chem. **89**, 897 (1985).
[27] R. Bohm, H. Morgner, J. Oberbrodhage, and M. Wulf, Surf. Sci. **317**, 407 (1994).
[28] M. Faubel, B. Steiner, and J. P. Toennies, J. Chem. Phys. **106**, 9013 (1997).
[29] P. Delahay, Acc. Chem. Res. **15**, 40 (1982).
[30] J. V. Coe, G. H. Lee, J. G. Eaton, S. T. Arnold, H. W. Sarkas, K. H. Bowen, C. Ludewigt, H. Haberland, and D. R. Worsnop, J. Chem. Phys. **92**, 3980 (1990).
[31] R. N. Pribble and T. S. Zwier, Science **265**, 75 (1994).
[32] C. J. Gruenloh, J. R. Carney, C. A. Arrington, T. S. Zwier, S. Y. Fredericks, and K. D. Jordan, Science **276**, 1678 (1997).
[33] X. B. Wang, X. Yang, J. B. Nicholas, and L. S. Wang, J. Chem. Phys. **116**, 561 (2002).
[34] C. F. Ding, X. B. Wang, and L. S. Wang, J. Phys. Chem. A **102**, 8633 (1998).
[35] X. B. Wang, J. B. Nicholas, and L. S. Wang, J. Chem. Phys. **113**, 10837 (2000).
[36] X. B. Wang, X. Yang, J. B. Nicholas, and L. S. Wang, Science **294**, 1322 (2001).
[37] X. Yang, X. B. Wang, and L. S. Wang, J. Phys. Chem. A **106**, 7607 (2002).
[38] J. M. Herbert and J. V. Ortiz, J. Phys. Chem. A **104**, 11786 (2000).
[39] L. S. Wang, C. F. Ding, X. B. Wang, and S. E. Barlow, Rev. Sci. Instrum. **70**, 1957 (1999).
[40] A. D. Becke, J. Chem. Phys. **98**, 5648 (1993).
[41] N. Godbout, D. R. Salahub, J. Andzelm, and E. Wimmer, Can. J. Chem. **70**, 560 (1992).
[42] R. A. Kendall, T. H. Dunning, Jr., and R. A. Harrison, J. Chem. Phys. **96**, 6796 (1992).
[43] T. H. Dunning, Jr., J. Chem. Phys. **90**, 1007 (1989).
[44] M. J. Frisch *et al.*, GAUSSIAN 98, Revision A (Gaussian, Inc., Pittsburgh, Pennsylvania, 1998).
[45] X. Yang, X. B. Wang, and L. S. Wang (unpublished).
[46] L. S. Wang and X. B. Wang, J. Phys. Chem. A **104**, 1978 (2000).
[47] X. B. Wang, C. F. Ding, and L. S. Wang, Phys. Rev. Lett. **81**, 3551 (1998).
[48] X. B. Wang, C. F. Ding, and L. S. Wang, Chem. Phys. Lett. **307**, 391 (1999).
[49] L. S. Wang, C. F. Ding, X. B. Wang, and J. B. Nicholas, Phys. Rev. Lett. **81**, 2667 (1998).
[50] D. Schröder and H. Schwarz, J. Phys. Chem. A **103**, 7385 (1999).
[51] X. Yang, X. B. Wang, and L. S. Wang, J. Chem. Phys. **115**, 2889 (2001).
[52] J. Dietter and H. Morgner, Chem. Phys. **220**, 261 (1997).
[53] I. Rips and J. Jortner, J. Chem. Phys. **97**, 536 (1992).
[54] R. N. Barnett, U. Landman, C. L. Cleveland, and J. Jortner, Chem. Phys. Lett. **145**, 382 (1988).
[55] R. A. Crowell and D. M. Bartels, J. Phys. Chem. **100**, 17940 (1996).
[56] B. J. Schwartz and P. J. Rossky, J. Chem. Phys. **101**, 6917 (1994).
[57] C. Silva, P. K. Walhout, K. Yokoyama, and P. F. Barbara, Phys. Rev. Lett. **80**, 1086 (1998).